Reconstitution of COPII vesicle fusion to generate a pre-Golgi intermediate compartment

Dalu Xu and Jesse C. Hay

Department of Molecular, Cellular and Developmental Biology, University of Michigan, Ann Arbor, MI 48109

What is the first membrane fusion step in the secretory pathway? In mammals, transport vesicles coated with coat complex (COP) II deliver secretory cargo to vesicular tubular clusters (VTCs) that ferry cargo from endoplasmic reticulum exit sites to the Golgi stack. However, the precise origin of VTCs and the membrane fusion step(s) involved have remained experimentally intractable. Here, we document in vitro direct tethering and SNARE-dependent fusion of endoplasmic reticulum–derived COPII transport vesicles to form larger cargo containers. The assembly did not require detectable Golgi membranes, preexisting VTCs, or COPI function. Therefore, COPII vesicles appear to contain all of the machinery to initiate VTC biogenesis via homotypic fusion. However, COPI function enhanced VTC assembly, and early VTCs acquired specific Golgi components by heterotypic fusion with Golgi-derived COPI vesicles.

Introduction

Vesicular tubular clusters (VTCs) were originally described as heterogeneous membranes distributed between ER exit sites and Golgi stacks (Schweizer et al., 1990; Saraste and Svensson, 1991; Bannykh et al., 1996). Later, VTCs were demonstrated to represent the primary vehicle for cargo transport from ER to Golgi (Presley et al., 1997; Scales et al., 1997) and to play a role in sorting of proteins back to the ER and selective concentration of anterograde cargo (Martinez-Menarguez et al., 1999). Until now, biochemical studies of ER-to-Golgi transport have focused on the fusion of ER-derived coat complex (COP) II vesicles with the cis-Golgi (Rowe et al., 1998). Thus, the subcellular origin of VTCs and the fusion event(s) that create them have remained speculative. The simplest model of VTC biogenesis assumes that VTCs arise by homotypic fusion of COPII vesicles. However, whether COPII vesicles possess the machinery for homotypic fusion has never been demonstrated. Because little experimental attention has been given to VTC biogenesis despite their central role in the secretory pathway, we sought to reproduce the process in test tube assays where the membrane fusion reactions could be precisely identified and probed.

Results and discussion

ER-to-Golgi transport is often studied in permeabilized mammalian cells (Rowe et al., 1998; Williams et al., 2004). Although a large majority of the model cargo, vesicular stomatitis virus glycoprotein (VSV-G) ts045, is transported to the Golgi under these conditions, the fusion events preceding arrival in the Golgi cannot be monitored. However, a portion of the COPII vesicles are released into the extracellular buffer during transport incubations (Joglekar et al., 2003), and these extracellular vesicles could potentially be monitored as they undergo pre-Golgi fusion events that would normally occur en route to the Golgi. Fig. 1 A demonstrates that this wayward vesicle pool carries 1.3% of epitope-tagged VSV-G-myc and is released from transfected semi-intact normal rat kidney (NRK) cells in a temperature-, energy-, cytosol-, and sar1-dependent process reflecting budding of COPII vesicles from the ER. A similar fraction of non–myc-tagged, radioactive VSV-G (VSV-G*) is released from another population of NRK cells that were infected with VSV and pulse radiolabeled. At the onset of the reaction, all VSV-G-myc and VSV-G* are present in the ER, because high-level expression of the protein (VSV-G-myc) or pulse labeling (VSV-G*) is accomplished at 40°C, a temperature at which VSV-G ts045 is retained in the ER. The initial ER restriction of the cargo, together with the inhibition by GDP-locked sar1 T39N and stimulation by wild-type sar1 indicates that a large majority of the released VSV-G is present in COPII vesicles. This population of vesicles contains four ER–Golgi SNAREs (Xu et al., 2000; Joglekar et al., 2003), as well as the vesicle marker p24 (Fig. S1 A, available at http://www.jcb.org/cgi/content/full/jcb.200408135/DC1). The cytoplasmically dis-
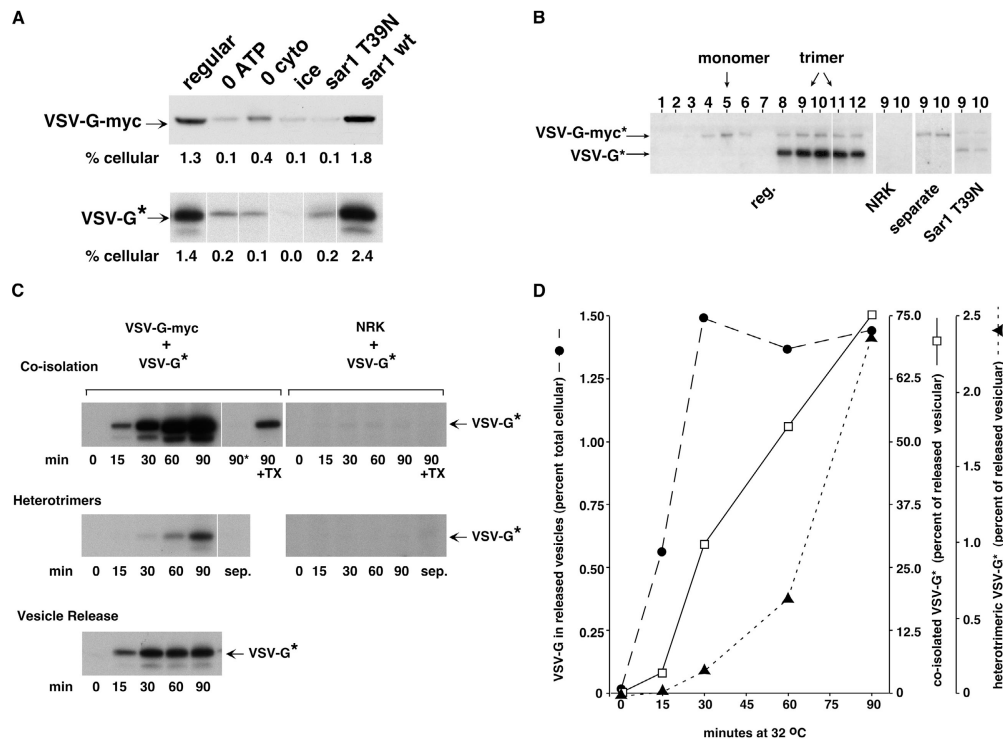
Figure 1. **Assembly of pre-Golgi intermediates in vitro.** Two populations of permeabilized cells were prepared containing ER-restricted VSV-G ts045: one was transfected with VSV-G-myc; the other was infected with VSV and pulse radiolabeled. After incubating the cells under various conditions, cells were removed by centrifugation at 15,000 g, and sedimentable vesicles in the supernatant were analyzed. (A) Release of vesicular VSV-G-myc (top, anti-myc immunoblot) and radioactive VSV-G* (bottom, autoradiogram) from separate cell populations. Purified sar1 proteins were added at 0.8–1.0 µM for this and subsequent experiments. Released vesicles were either directly sedimented at 100,000 g (top) or immunoisolated using anti-p24 antibody (bottom). (A–C) White lines indicate that intervening lanes have been spliced out. (B) Sedimentation analysis of VSV-G-myc* and VSV-G* present on released vesicles after coincubation of the two cell populations. Vesicles were solubilized with Triton X-100 before gradient. After sedimentation, gradient fractions were subjected to immunoprecipitation with anti-myc antibody and analyzed by autoradiography. In this and subsequent figures, "NRK" reactions contained nontransfected cells instead of VSV-G-myc* cells, but did contain regular VSV-G* cells. (C) Time course analysis of vesicle coisolation (top), heterotrimer formation (middle), and vesicle release (bottom) by autoradiography. 90*, centrifuged at 100,000 g before immunoisolation; 90 + TX, immunoisolation of vesicles followed by washing of immunobeads with Triton X-100; Sep., the two populations were incubated separately, and then combined before detergent solubilization. (D) Quantitation of the results from C. Vesicle release from semi-intact cells is expressed relative to the total cellular pool of VSV-G*. Coisolation and heterotrimer formation are expressed as a percentage of released vesicular pool.

posed myc epitope of VSV-G-myc allows immunoisolation of cargo-loaded vesicles with ∼25% efficiency (Fig. S1 B).

To determine whether the released vesicles can recapitulate pre-Golgi intermediate formation, we incubated both populations of permeabilized NRK cells together under transport conditions for varying times, removed the cells by centrifugation at 15,000 g, immunoisolated VSV-G-myc–containing vesicles from the supernatant, and examined coisolation of VSV-G*–containing vesicles by autoradiography. Under these conditions, VSV-G* coisolation would be indicative of tethering and/or fusion of vesicles released from different cells. Fig. 1 C (top left) shows that VSV-G* was specifically coisolated in a time- and temperature-dependent process. The coisolated cargo was vesicle bound because prior high-speed centrifugation eliminated coisolation (Fig. 1 C, 90*). The coisolation was immune specific because VSV-G-myc transfection was essential (Fig. 1 C, top right).

Although coisolation could be indicative of tethering and/or fusion, it cannot distinguish between these possibilities. To specifically examine fusion, we exploited the rapid equilibrium between VSV-G trimers and monomers (Zagouras and Rose,

1993). When COPII vesicles have fused, but not when they have only tethered, this rapid equilibrium will promote heterotrimers that contain at least one subunit each of VSV-G-myc and VSV-G*. As shown in Fig. 1 C (top left, 90 + TX), when coisolated, bead-immobilized vesicles were solubilized with detergent, most of the VSV-G* was removed but ∼15% remained bound. We anticipated that this 15% represented heterotrimers formed after COPII vesicle fusion. To confirm the presence of heterotrimers, we established conditions for velocity sedimentation of solubilized membranes that separates VSV-G monomers and trimers (Fig. S1 C). Then, by radiolabeling both the VSV-G-myc–transfected and VSV-infected populations of NRK cells, we were able to analyze the distribution of VSV-G-myc–containing species present on released COPII vesicles. As shown in Fig. 1 B, ∼25% of VSV-G-myc* was present in the monomer peak and ∼75% in the trimer peak. The myc immunoprecipitations revealed that only the trimer peak contained coprecipitable VSV-G*, confirming the presence of heterotrimers. Importantly, when the two populations of NRK cells were incubated separately at 32°C and combined just before the vesicles were solubilized, no hetero-
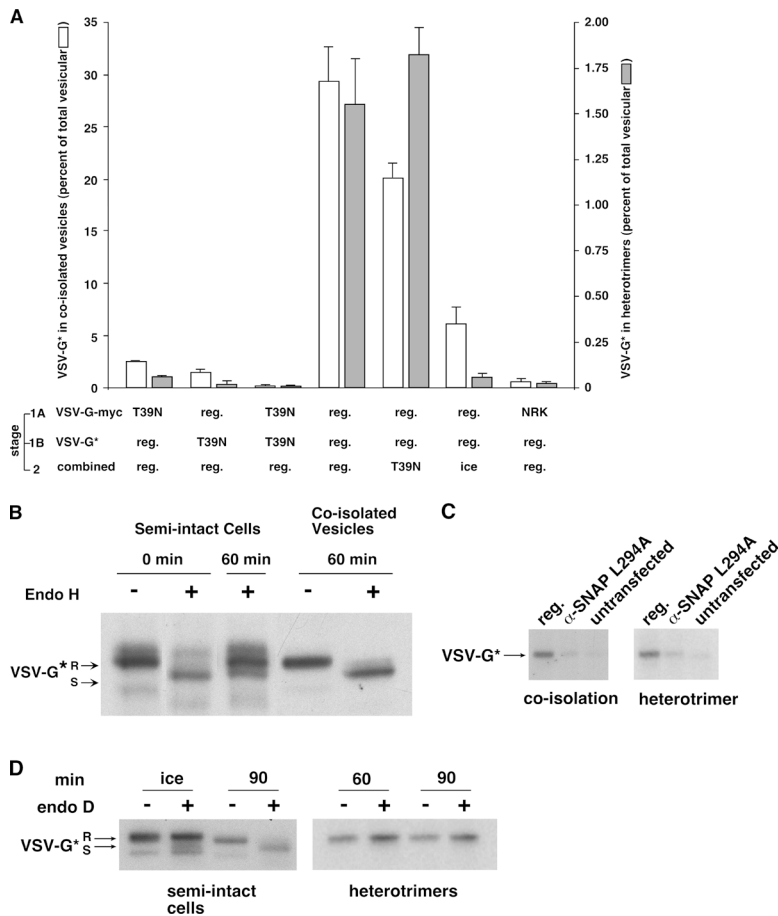
Figure 2. **Assembly involves symmetric populations of COPII vesicles but not Golgi.** (A) Released VSV-G-myc vesicles and VSV-G* vesicles were prepared separately, semi-intact cells were removed, and the vesicles were combined for second-stage incubations. After the second incubation, vesicles were analyzed for coisolation and heterotrimer formation as in Fig. 1. Purified recombinant sar1 T39N was included at different points. (A) Error bars represent the SEM of duplicate determinations. (B) Single-stage coisolation assay was performed as in Fig. 1. The coisolated vesicles, as well as samples of semi-intact cells from before and after the incubation were subjected to digestion with endo H and analyzed by autoradiography. R and S represent resistant and sensitive bands, respectively. (C) Single-stage coisolation and heterotrimer assays using CHO 15B cells. The α-SNAP L294A reaction contained 5 μM of recombinant protein. (D) Single-stage heterotrimer assay was performed as in C. Immunoprecipitated heterotrimers as well as samples of semi-intact cells from before and after the incubation were subjected to digestion with endo D and analyzed by autoradiography.

trimers were present (Fig. 1 B, separate), demonstrating that heterotrimers do not form in detergent. Finally, the appearance of heterotrimers was COPII dependent (Fig. 1 B, Sar1 T39N).

We analyzed the time course of heterotrimer formation using unlabeled VSV-G-myc cells incubated together with radiolabeled VSV-G* cells. As shown in Fig. 1 C (middle), heterotrimer formation was completely time and incubation dependent. In this standardized assay, heterotrimers were specifically immunoprecipitated (Fig. 1 C, right) and did not form during the detergent steps (Fig. 1 C, left, sep.). Fig. 1 C (bottom) shows the time course of release of vesicular VSV-G*, irrespective of tethering or fusion. Quantitation of the results for vesicular VSV-G* release, vesicle coisolation, and heterotrimer formation is shown in Fig. 1 D. Vesicle release is a rapid process that reaches its maximal by 30 min; in contrast, coisolation exhibits a lag of 15 min, and heterotrimer formation, a lag of >30 min. These kinetics are consistent with three sequential, dependent processes of vesicle budding, tethering, and fusion, although heterotrimerization may exhibit a lag after vesicle fusion. Vesicle coisolation is a robust process, with up to 75% efficiency; heterotrimer formation was less efficient (2.5%), although this may be caused by inefficient subunit mixing as opposed to inefficient fusion. Vesicle coisolation exhibited a biphasic sensitivity to vesicle concentration (Fig. S2, available at http://www.jcb.org/cgi/content/full/jcb.200408135/DC1). The inhibition by dilution can be explained by the requirement for diffusing vesicles to encounter one another; the inhibition by concentration can be explained by very efficient fusion resulting in large intermediates that sediment when the cells are removed. Thus, our assays are poised to measure the initial steps in VTC assembly. Although the percentage of total cellular VSV-G that participates in the "extracellular" process we monitor is small, we believe that the released vesicles reflect the behavior of intracellular pre-Golgi structures (Fig. S3, available at http://www.jcb.org/cgi/content/full/jcb.200408135/DC1).

The aforementioned experiments involved coincubation of both donor cell populations in one tube and preclude analysis of the individual fusion partners. To overcome this limitation, we used a two-stage protocol in which VSV-G-myc–containing vesicles and VSV-G*–containing vesicles were obtained in separate vesicle release incubations, and then combined to allow tethering and fusion during a second incubation. As shown in Fig. 2 A, both vesicle coisolation (open bars) and heterotrimer formation (shaded bars) displayed symmetric requirements for COPII-packaged cargo, because sar1 T39N fully inhibited tethering and fusion when included during either first-stage incubation. This rules out the possibility that our assays depend on fusion of COPII vesicles with ER fragments released from semi-intact cells. Furthermore, the functional requirement for COPII packaging occurs during the first stage only, because sar1 T39N addition during stage 2 is ineffective.
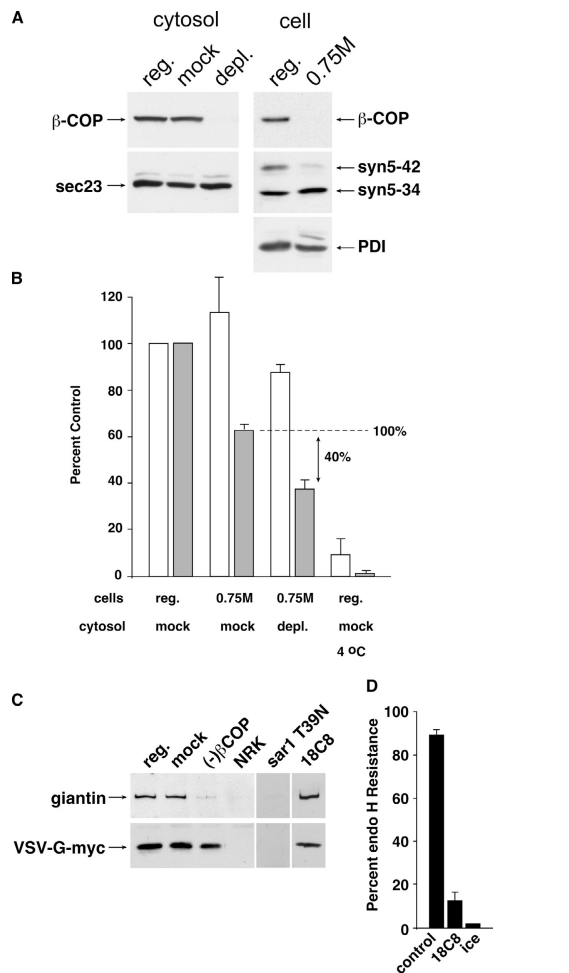
Figure 3. **Golgi-derived COPI vesicle fusion with pre-Golgi intermediates stimulates, but is not required for assembly.** (A) Immunoblot before and after immunodepletion or mock immunodepletion of liver cytosol (left) and before and after 0.75 M KCl extraction of semi-intact NRK cells (right). (B) Single-stage vesicle coisolation (open bars) and heterotrimer (shaded bars) assays were performed using the indicated combinations of cells and cytosol. The double-headed arrow represents the 40% decrease specifically caused by deletion of COPI from the cytosol. (C) KCl-extracted VSV-G-myc–transfected NRK cells were incubated in the presence of regular-, mock-, or β-COP–depleted cytosol, or mock-depleted cytosol containing sar1 T39N, or 1.25 μM of purified 18C8. Released vesicles were immunoisolated using anti–myc antibodies and immunoblotted using anti–VSV-G and antigiantin antibodies. (D) ER-to-Golgi transport of VSV-G* monitored by endo H resistance in the presence or absence of 1.25 μM 18C8. Error bars in B and D represent the SEM of duplicate determinations.

A portion of the coisolation signal is obtained from vesicles held on ice during stage 2; this result is consistent with a tethered, unfused intermediate. Heterotrimer formation was completely inhibited on ice, as expected for membrane fusion.

Although the symmetric requirement for COPII vesicles was consistent with homotypic fusion, it did not rule out the possibility that two populations of COPII vesicles fused with common Golgi fragments. As shown in Fig. 2 B, whereas VSV-G* retained within semi-intact cells progresses from sensitive to endoglycosidase (endo) H to resistant within 60 min of incubation, the VSV-G* on coisolated vesicles remains entirely sensitive to endo H. Thus, the coisolated pool of VSV-G* does not come in contact with cis/medial-Golgi
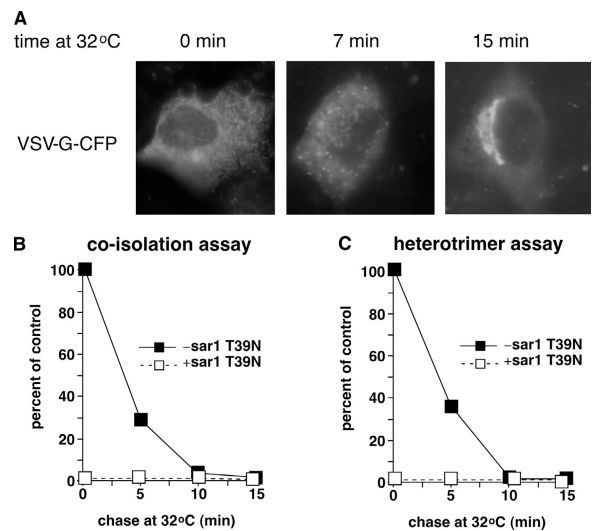

Figure 4. **Preexisting pre-Golgi intermediates do not tether and fuse with COPII vesicles released from permeabilized cells.** (A) NRK cells were transfected with VSV-G-CFP and incubated at 40°C. Cells were incubated for the indicated times at 32°C before fixation and fluorescence microscopy. (B and C) Two-stage coisolation or heterotrimer assays were conducted using the usual VSV-G-myc vesicles together with VSV-G* vesicles from cells that had been preincubated at 32°C for the indicated times before permeabilization. The first-stage incubation of the chased cells was conducted with or without sar1 T39N. To differentiate the potential involvement of preexisting VTCs from a role for COPI vesicles as defined in Fig. 3, these assays were conducted under COPI-free conditions.

enzymes, which is consistent with a pre-Golgi nature. In CHO 15B cells, exposure of glycans to mannosidase I imparts sensitivity to endo D (Rowe et al., 1998). Fig. 2 C shows that CHO15B cells can be adapted for analysis of vesicle coisolation and heterotrimerization. Fig. 2 D illustrates that whereas VSV-G* retained within semi-intact CHO 15B cells becomes completely endo D sensitive within 90 min, released heterotrimers remain entirely endo D resistant. Thus, by biochemical criteria, the fusion intermediates in our system represent bona fide pre-Golgi structures that lack even the earliest cis-Golgi enzymes.

The data presented so far are consistent with VTC formation occurring by homotypic fusion of COPII vesicles, but does not exclude involvement of other vesicles. Because only COPII and COPI vesicles are known to function in ER-to-Golgi transport, we wanted to investigate whether COPI vesicles contributed to in vitro VTC formation. Anti–β-COP antibody was used to deplete this essential COPI subunit from rat liver cytosol (Fig. 3 A, left lanes). Washed semi-intact cells contained significant β-COP that could be extracted completely with 0.75 M KCl (Fig. 3 A, right lanes). Thus, we were able to completely deplete our system of COPI and examine the effects on pre-Golgi vesicle events. Salt-stripped semi-intact cells were fully functional for vesicle coisolation in the presence of COPI-containing cytosol (Fig. 3 B, first two open bars). However, these cells were 37% less active in the heterotrimer assay (Fig. 3 B, first two shaded bars), indicating that additional components may have been damaged or extracted. Hence, 63% of the control value should be considered maximal for the heterotrimer assay with salt-stripped cells. When the salt-stripped cells
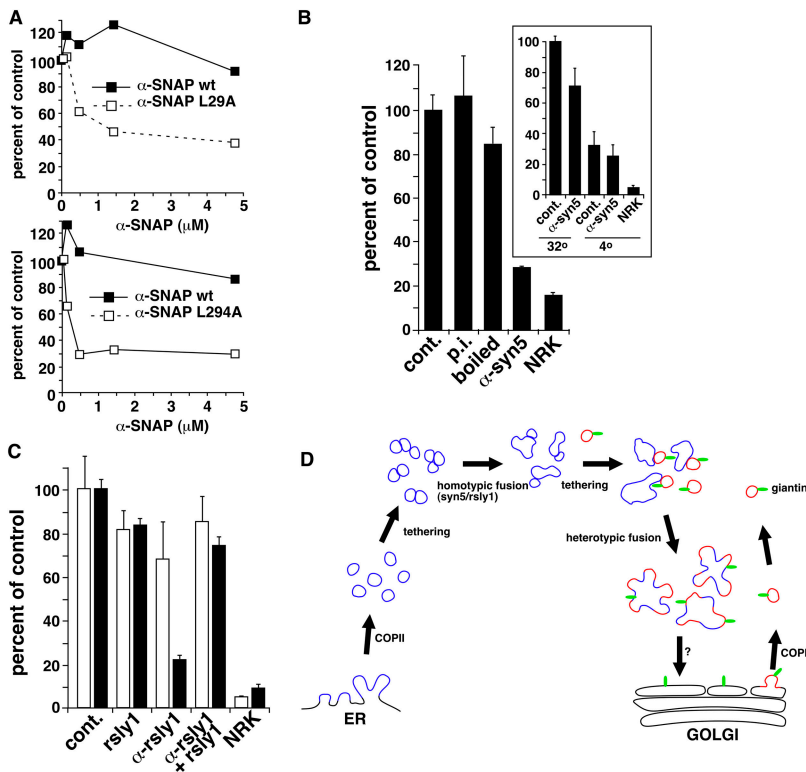
Figure 5. NSF, syntaxin 5, and rsly1 are required for homotypic fusion of COPII vesicles. (A) Two-stage VSV-G* coisolation (top) and heterotrimer (bottom) assays were conducted in the presence of increasing concentrations of wild-type or α-SNAP L294A. (B) Two-stage heterotrimer assay was conducted under COPI-free conditions in the presence of 130 nM of control rabbit IgG or affinity-purified polyclonal anti–syntaxin 5 antibodies, either native or boiled. (inset) Two-stage coisolation assay using anti–syntaxin 5 antibody at the same concentrations. (B and C) Error bars represent the SEM of duplicate determinations. (C) Two-stage coisolation (open bars) and heterotrimer (shaded bars) assays were conducted under COPI-free conditions in the presence of GST-rsly1–purified protein and 267 nM anti-rsly1 antibodies. (D) Model of in vitro VTC biogenesis and maturation (Results and discussion).

were combined with COPI-depleted cytosol, the coisolation assay was marginally affected and the heterotrimer assay was 60% active relative to maximal for salt-stripped cells (Fig. 3 B, third and fourth bars vs. fifth and sixth bars). Thus, COPI-dependent processes do contribute to pre-Golgi fusion events, perhaps by provision of fusion machinery limiting on COPII vesicles. However, they are not an essential component of in vitro VTC formation.

Another possibility would be that the two populations of COPII vesicles fused in common with preexisting VTCs or another pre-Golgi structure. The putative intervening membrane would also be released from the cells during the first stage of incubation and act as a bridge between COPII vesicles. Thus, if this compartment were first loaded with one of the differently tagged VSV-G, we should be able to detect tethering and/or fusion of this membrane with COPII vesicles containing the other tagged VSV-G. As shown in Fig. 4 A, CFP-tagged VSV-G that is initially locked in the ER moves into VTCs and then to the Golgi during a 0–15-min preincubation of intact cells at the permissive temperature. Importantly, Fig. 4 (B and C) shows that as VSV-G*–containing cells are similarly preincubated before permeabilization, the capacity for coisolation and heterotrimerization with VSV-G-myc–containing COPII vesicles is rapidly lost. No assay signal is obtained when the progressively chased cell population is incubated with sar1 T39N during the vesicle release stage. Thus, only VSV-G* in COPII vesicles directly released from the ER can tether and fuse with VSV-G-myc in COPII vesicles; putative post-ER secretory intermediates such as preexisting VTCs are either not released during the incubation or cannot interact with COPII vesicles. Based on Figs. 3 (A and

B) and 4, it would appear that pre-Golgi intermediates, at least in vitro, are built primarily by homotypic COPII vesicle fusion. On the other hand, a formal possibility remains that an unrelated membrane intervenes to mediate fusion between COPII vesicles.

Because COPI vesicles contribute to pre-Golgi cargo carrier formation (Fig. 3 B), it may be possible to detect recruitment of early Golgi markers. As shown in Fig. 3 C, immunoisolated cargo carriers from salt-stripped cells in COPI-containing cytosol contained the cis-Golgi integral membrane protein giantin, which is thought to participate in tethering of intra-Golgi vesicles and Golgi assembly (Sonnichsen et al., 1998). However, when the assay was performed in COPI-depleted cytosol, giantin was absent from the fusion intermediates. Inclusion of sar1 T39N also eliminated giantin-and-VSV-G-myc–containing intermediates, demonstrating that the relevant cargo was released from the ER during the incubation. These results imply that giantin is delivered to nascent VTCs from the Golgi via COPI vesicles, but does not rule out that the relevant VSV-G-myc was first delivered to the Golgi, and then budded in COPI vesicles. We addressed this possibility using a monoclonal antibody, 18C8, that recognizes the free but not the complexed syntaxin 5 SNARE motif (Williams et al., 2004). Although 18C8 completely inhibits ER-to-Golgi transport in the donor cells (Fig. 3 D), it has little or no effect on COPII vesicle coisolation, heterotrimer formation (not depicted), or giantin recruitment (Fig. 3 C). Thus, we were able to functionally uncouple ER-to-Golgi transport from giantin recruitment to pre-Golgi intermediates, further supporting COPI–COPII vesicle fusion as the mechanism. The explanation for the lack of inhibition

of vesicle fusion by 18C8 likely relates to relative inaccessibility of the vesicular syntaxin 5 SNARE motif compared with other pools of syntaxin 5 (e.g., in the Golgi), required for complete ER-to-Golgi transport. In summary, the results of Fig. 3 (A–D) indicates that heterotypic fusion between COPII-based cargo containers and retrograde COPI vesicles stimulates more fusion with COPII vesicles and recruits a subset of cis-Golgi components. The contributing COPI pathway appears to be selective because it does not carry Golgi enzymes such as mannosidase I (Fig. 2).

A mammalian ER–Golgi SNARE complex has been well-characterized and documented to function in transport (Xu et al., 2000; Williams et al., 2004), but the precise fusion event it catalyzes is unresolved. SNAREs were required for assembly of nascent VTCs because dominant-negative α-SNAP L294A (Barnard et al., 1997) inhibited both vesicle coisolation and heterotrimer formation, with a more potent and complete inhibition of the latter (Fig. 5 A). Significant inhibition of coisolation was unexpected because SNAREs are not known to function in tethering. One potential explanation is that dissociation of cis-SNARE complexes by NSF may be required to recruit or activate the tethering machinery. Fig. 5 B shows that polyclonal antibodies against syntaxin 5, the Q_A-SNARE for the ER–Golgi quaternary complex, inhibited the two-stage heterotrimer formation assay. Unlike the 18C8 monoclonal antibody used in Fig. 3, this anti–syntaxin 5 antiserum recognizes free as well as the cis-complexed syntaxin 5 (Williams et al., 2004) and inhibits a broader range of its functions. This experiment was conducted under COPI-free conditions, thus the results demonstrate that syntaxin 5 is required for the homotypic fusion of COPII vesicles to form early VTCs. As expected for a SNARE involved specifically in membrane fusion, syntaxin 5 inhibition had only minor effects on the vesicle coisolation assay performed in parallel (inset). Fig. 5 C shows that polyclonal antibodies against rsly1, the SM protein inextricably linked to syntaxin 5 function (Williams et al., 2004), specifically inhibited the two-stage heterotrimer assay under COPI-free conditions without significant effect on vesicle coisolation, suggesting a post-docking action close to membrane fusion. These results establish that the syntaxin 5–SNARE complex and rsly1 function in the earliest pre-Golgi membrane fusion event that appears to involve homotypic fusion of COPII vesicles.

Fig. 5 D presents a model for VTC biogenesis and maturation based on our findings. Cargo-containing COPII vesicles undergo homotypic tethering and fusion to form nascent VTCs. The ER–Golgi quaternary SNARE complex containing syntaxin 5 and the SM protein rsly1 appear to mediate this fusion. Although not required for initial cargo container assembly, retrograde COPI vesicles appear to stimulate this process, perhaps by provision of additional tethering and/or fusion machinery; these vesicles carrying giantin undergo heterotypic fusion with either COPII vesicles (not depicted) and/or nascent VTCs. In the cell, this COPI retrograde pathway may contribute to the maturation of VTCs into a cis-Golgi network that later becomes cis-Golgi.

Materials and methods

Transfection, virus infection, ^{35}S labeling, and cell permeabilization
Expression of VSV-G-myc was accomplished by a combination of transfection and vaccinia virus infection. A 10-cm plate of NRK cells were transfected with VSV-G-myc by electroporation. The next day, the NRK cells were infected with recombinant vaccinia virus containing the gene for phage T7 RNA polymerase and incubated at 40°C for 5–6 h to allow high-level VSV-G-myc expression. Meanwhile, a 10-cm plate of NRK cells was infected with vesicular stomatitis virus strain ts045 and incubated for 4 h at 32°C. The VSV-infected plate was then transferred to a 40°C water bath, starved with cysteine/methionine-free medium, and radiolabeled for 10 min as described previously (Williams et al., 2004) with 500 μCi of ^{35}S-cysteine/methionine. To prepare permeabilized cells for vesicle trafficking assays, both types of virus-infected cells were washed and gently scraped from the plate using a rubber policeman. Scrape-permeabilized cells were washed once by centrifugation/resuspension and resuspended in 100 μl of 50/90 buffer (50 mM Hepes, pH 7.2, and 90 mM potassium acetate) per 10-cm plate of cells.

Coisolation and heterotrimerization assays
For one-stage assays, each reaction mixture contained 200 μl and consisted of the following: 55 μl of 25/125 buffer (25 mM Hepes, pH 7.2, and 125 mM potassium acetate) or antibodies/proteins dissolved in 25/125, 32 μl of water, 5 μl of 0.1 M magnesium acetate, 10 μl of ATP-regenerating system, 3 μl of 1 M Hepes, pH 7.2, 20 μl of a solution of 50 mM EGTA, 18 mM CaCl$_2$, and 20 mM Hepes, pH 7.2, 50 μl of rat liver cytosol dialyzed into 25/125, 12.5 μl of semi-intact NRK cells transfected with VSV-G-myc, and 12.5 μl of semi-intact NRK cells infected with VSV and ^{35}S-labeled. Reaction mixtures were incubated at 32°C for 90 min, centrifuged at 4,000 g for 1 min followed by 15,000 g for 1 min, and the supernatant was saved for analysis.

For two stage assays, first-stage reaction mixtures contained the same concentrations of the above contents in 100 μl total and either 12.5 μl of VSV-G-myc–transfected cells or 12.5 μl of VSV-infected radiolabeled cells, but not both. After incubating at 32°C for 30 min, cells were removed by centrifugation as above, and the supernatants from the two kinds of cells were combined and incubated at 32°C for another 60 min.

For either the one-stage or two-stage assays, the final cell-free vesicle suspension was supplemented with 5 μg 9E10 mAb and mixed at 4°C overnight. The suspension was cleared at 4,000 g for 1 min followed by addition of 15 μl of (packed) protein A beads and further mixing at 4°C for 6 h. Beads were preblocked in 25/125 buffer containing 0.5 mg/ml dry nonfat milk and 0.5 mg/ml PVP-40T. When test antibodies were added to the vesicle assays (Fig. 5 and Fig. S3 [available at http://www.jcb.org/cgi/content/full/jcb.200408135/DC1]), we used biotinylated mAb 9E10 and streptavidin beads instead of protein A beads. After the incubations, beads were washed four times by centrifugation and resuspended in 25/125 buffer. Proteins were eluted from protein A–Sepharose beads by the addition of 0.1 M glycine, pH 2.5, neutralized and concentrated by ultrafiltration, and analyzed by 8% SDS-PAGE and autoradiography.

For heterotrimer assays, reaction mixtures were prepared and incubated as in previous paragraphs; however, the final vesicle suspensions were supplemented with 2% Triton X-100 for 20 min, followed by centrifugation at 100,000 g for 30 min. The 100,000-g supernatants were subjected to immunoprecipitation as in previous paragraph.

Image acquisition
Microscopic images were collected at room temperature using a microscope (model E-800; Nikon) equipped with a 60x/1.4 Plan Apo objective, filter cubes for CFP and YFP fluorescence, and a camera (ORCA II; Hamamatsu), controlled by Improvision Openlab software. Image cropping and adjustment were accomplished using Photoshop (Adobe).

Online supplemental material
Fig. S1 shows analysis of transport vesicles from semi-intact NRK cells. Fig. S2 shows the cell concentration dependence of vesicle release and coisolation. Fig. S3 shows that vesicles normally retained within semi-intact cells can undergo homotypic interactions. Supplemental materials and methods provides details of the antibodies used, a description of DNA plasmids, as well as details of the endoglycosidase analyses, velocity sedimentation methods, and the analysis of giantin recruitment to nascent VTCs. Fig. S1–S3 and legends as well as Supplemental materials and methods are available at http://www.jcb.org/cgi/content/full/jcb.200408135/DC1.

References

Bannykh, S.I., T. Rowe, and W.E. Balch. 1996. The organization of endoplasmic reticulum export complexes. *J. Cell Biol.* 135:19–35.

Barnard, R.J., A. Morgan, and R.D. Burgoyne. 1997. Stimulation of NSF ATPase activity by alpha-SNAP is required for SNARE complex disassembly and exocytosis. *J. Cell Biol.* 139:875–883.

Joglekar, A.P., D. Xu, D.J. Rigotti, R. Fairman, and J.C. Hay. 2003. The SNARE motif contributes to rbet1 intracellular targeting and dynamics independently of SNARE interactions. *J. Biol. Chem.* 278:14121–14133.

Martinez-Menarguez, J.A., H.J. Geuze, J.W. Slot, and J. Klumperman. 1999. Vesicular tubular clusters between the ER and Golgi mediate concentration of soluble secretory proteins by exclusion from COPI-coated vesicles. *Cell.* 98:81–90.

Presley, J.F., N.B. Cole, T.A. Schroer, K. Hirschberg, K.J. Zaal, and J. Lippincott-Schwartz. 1997. ER-to-Golgi transport visualized in living cells. *Nature.* 389:81–85.

Rowe, T., C. Dascher, S. Bannykh, H. Plutner, and W.E. Balch. 1998. Role of vesicle-associated syntaxin 5 in the assembly of pre-Golgi intermediates. *Science.* 279:696–700.

Saraste, J., and K. Svensson. 1991. Distribution of the intermediate elements operating in ER to Golgi transport. *J. Cell Sci.* 100:415–430.

Scales, S.J., R. Pepperkok, and T.E. Kreis. 1997. Visualization of ER-to-Golgi transport in living cells reveals a sequential mode of action for COPII and COPI. *Cell.* 90:1137–1148.

Schweizer, A., J.A. Fransen, K. Matter, T.E. Kreis, L. Ginsel, and H.P. Hauri. 1990. Identification of an intermediate compartment involved in protein transport from endoplasmic reticulum to Golgi apparatus. *Eur. J. Cell Biol.* 53:185–196.

Sonnichsen, B., M. Lowe, T. Levine, E. Jamsa, B. Dirac-Svejstrup, and G. Warren. 1998. A role for giantin in docking COPI vesicles to Golgi membranes. *J. Cell Biol.* 140:1013–1021.

Williams, A.L., S. Ehm, N.C. Jacobson, D. Xu, and J.C. Hay. 2004. rsly1 binding to syntaxin 5 is required for endoplasmic reticulum-to-Golgi transport but does not promote SNARE motif accessibility. *Mol. Biol. Cell.* 15:162–175.

Xu, D., A.P. Joglekar, A.L. Williams, and J.C. Hay. 2000. Subunit structure of a mammalian ER/Golgi SNARE complex. *J. Biol. Chem.* 275:39631–39639.

Zagouras, P., and J.K. Rose. 1993. Dynamic equilibrium between vesicular stomatitis virus glycoprotein monomers and trimers in the Golgi and at the cell surface. *J. Virol.* 67:7533–7538.